Featured in Physics

Hexapartite Entanglement in an above-Threshold Optical Parametric Oscillator

F. A. S. Barbosa,[1] A. S. Coelho,[2,3] L. F. Muñoz-Martínez,[4] L. Ortiz-Gutiérrez,[5]
A. S. Villar,[6] P. Nussenzveig,[7] and M. Martinelli[7,*]

[1]*Instituto de Física Gleb Wataghin, Universidade Estadual de Campinas, 13083-859 Campinas, São Paulo, Brazil*
[2]*Departamento de Engenharia Mecânica, Universidade Federal do Piauí, 64049-550 Teresina, Piauí, Brazil*
[3]*Departamento de Engenharia, Centro Universitário UNINOVAFAPI, 64073-505 Teresina, Piauí, Brazil*
[4]*Departamento de Ciencias Básicas, Universidad del Sinú-Elías Bechara Zainúm, Cra 1w # 38-153, Montería, Córdoba, Colombia*
[5]*Instituto de Física de São Carlos, Universidade de São Paulo, P.O. Box 369, 13560-970 São Carlos, São Paulo, Brazil*
[6]*American Physical Society, 1 Research Road, Ridge, New York 11961, USA*
[7]*Instituto de Física da Universidade de São Paulo, P.O. Box 66318, 05315-970 São Paulo, Brazil*

(Received 6 March 2018; published 13 August 2018)

We demonstrate, theoretically and experimentally, the generation of hexapartite modal entanglement by the optical parametric oscillator (OPO) operating above the oscillation threshold. We show that the OPO generates a rich structure of entanglement among sets of six optical sideband modes interacting through the nonlinear crystal. The class of quantum states thus produced can be controlled by a single parameter, the power of the external laser that pumps the system. Our platform allows for the generation of massive entanglement among many optical modes with well defined but vastly different frequencies, potentially bridging nodes of a multicolor quantum network.

DOI: 10.1103/PhysRevLett.121.073601

In the burgeoning field of quantum information science [1], entanglement is considered to be the greatest resource. This intrinsic quantum property, studied since the early days of quantum mechanics [2,3], can be generated in a number of physical systems and particularly in quantum optics, owing to the great control over optical systems and the high fidelity in the measurement of their observables.

One of the workhorses of the field, the continuously pumped triply resonant optical parametric oscillator (cw OPO), consists of a nonlinear crystal that couples three modes within a cavity (Fig. 1). The nonlinear coupling leads to the creation (and annihilation) of pairs of photons in down-converted fields (denoted 1 and 2, also known as signal and idler), with the annihilation (or creation) of a photon in the pump field 0. Since the pumped nonlinear crystal acts as a gain medium, when this gain matches the cavity losses, the system achieves an oscillatory regime with the generation of intense output beams. Controlling the pump power, we can explore a broad set of different quantum states of the field. Examples range from squeezed states for the down-converted mode [4] and the pump [5] to bipartite entanglement below [6] and above [7] the oscillation threshold, reaching tripartite entanglement involving fields spanning more than one octave in frequency [8].

Further steps are typically required to generate more intricate multipartite entangled states. For instance, off-cavity combinations of squeezed states and beam splitters lead to a two-rail cluster state generation in the time domain, presenting entanglement of more than 10 000 modes defined by multiplexing of a cw OPO output in time slices of 160 ns [9]. Alternatively, by manipulating the pairwise generation of entangled states in frequency modes separated by the cavity free spectral range, quadripartite entangled states [10], and a frequency comb of 60 modes separated by 1 GHz [11] were engineered. Multipartite entanglement was also generated with pulsed OPOs, leading to entanglement over the wide spectra of its output, as studied in 10 spectral modes in the range from 790 to 800 nm [12].

In this Letter, we show that, even without resorting to such techniques, a rich structure of multimode entangled states is already found in the cw triply resonant OPO pumped by a monochromatic field, in its operation above the oscillation threshold (Fig. 1). Starting from a driving field, with vacuum states for all the other modes, the system evolves to a hexapartite entangled state. This entanglement is found in the sideband modes of the intense fields of the reflected pump and the down-converted beams.

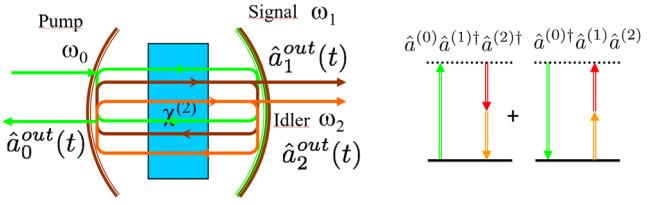

FIG. 1. The optical parametric oscillator consists of one triply resonant cavity with a nonlinear crystal that is responsible for coupling the pump field (0) to the signal (1) and idler (2) down-converted fields.

These modes are accessed by a combination of electronic demodulation of the measured photocurrents of the fields, with the help of empty cavities for each beam in a resonator detection technique [13]. Hexapartite entanglement is verified by tests of positivity under partial transposition [14]. In the following, we present the structure of the generated entangled states as well as their control by the pump power.

The evolution of the field operators $\hat{a}^{(n)}$ for each resonant cavity mode depends on the propagation inside the cavity, the coupling to external modes through the mirrors, and their coupling within the nonlinear crystal. The latter is described by an interaction Hamiltonian

$$\hat{H}_\chi = i\hbar\frac{\chi}{\tau}[\hat{a}^{(0)}(t)\hat{a}^{(1)\dagger}(t)\hat{a}^{(2)\dagger}(t) - \text{H.c.}], \tag{1}$$

where χ is the effective second order susceptibility, τ is the time of flight through the medium, and field indices 0, 1, and 2 stand for pump, signal, and idler modes, respectively. The OPO has been studied in detail for decades [15], and it is usually treated by the time evolution of these field operators $\hat{a}^{(n)}$ or by the evolution of the density operator in a suitable quasiprobability representation. These treatments lead to an effective three-mode description of the problem.

Nevertheless, a careful analysis of the measurement technique [16] reveals that the measured state of the output modes involves information of the two sideband modes for each carrier field. The role of each individual sideband is clear if we consider that each annihilation operator of the field $\hat{a}^{(n)}(t)$ is associated with the electric field operator of a propagating wave, which can be described by the sum of time independent field operators as $\hat{a}^{(n)}(t) = e^{-i\omega_n t}\int_{-\omega_n}^{\infty} d\Omega e^{-i\Omega t}\hat{a}^{(n)}_{\omega_n+\Omega}$, where $\hat{a}_\omega$ is the photon annihilation operator in the mode of frequency $\omega = \omega_n + \Omega$, and the carrier frequency ω_n is put in evidence. On the detection of the output fields, we access the information on the sideband modes, shifted by Ω from the carrier [13,16].

The interaction Hamiltonian can be rewritten using a linearized version of the field operators in the rotating frame, detailing the role of the sideband modes. In this linearized description, the field operator is replaced by its mean value $\alpha_{\omega_n} = \langle\hat{a}^{(n)}(t)e^{i\omega_n t}\rangle = \langle\hat{a}^{(n)}_{\omega_n}\rangle$ and a fluctuation term $\delta\hat{a}^{(n)}(t) = \hat{a}^{(n)}(t)e^{i\omega_n t} - \alpha_{\omega_n}$. If we retain only the terms satisfying the rotating wave approximation and neglect those without the contribution of the intense field amplitudes α_{ω_n}, we have the Hamiltonian involving the specific sideband modes of the three carriers, with $\Omega > 0$,

$$\begin{aligned}\hat{H}_\chi(\Omega) = -i\hbar\frac{\chi}{\tau}[&\alpha^*_{\omega_0}(\hat{a}^{(1)}_{\omega_1+\Omega}\hat{a}^{(2)}_{\omega_2-\Omega} + \hat{a}^{(1)}_{\omega_1-\Omega}\hat{a}^{(2)}_{\omega_2+\Omega})\\ &+ \alpha_{\omega_1}(\hat{a}^{(0)\dagger}_{\omega_0+\Omega}\hat{a}^{(2)}_{\omega_2+\Omega} + \hat{a}^{(0)\dagger}_{\omega_0-\Omega}\hat{a}^{(2)}_{\omega_2-\Omega})\\ &+ \alpha_{\omega_2}(\hat{a}^{(0)\dagger}_{\omega_0+\Omega}\hat{a}^{(1)}_{\omega_1+\Omega} + \hat{a}^{(0)\dagger}_{\omega_0-\Omega}\hat{a}^{(1)}_{\omega_1-\Omega}) - \text{H.c.}],\end{aligned} \tag{2}$$

where we have discarded the constant term $(\alpha^*_{\omega_0}\alpha_{\omega_1}\alpha_{\omega_2} - \text{c.c.})$, which will just introduce a global phase. Linear terms like $\alpha^*_{\omega_0}\alpha_{\omega_1}\hat{a}^{(2)}_{\omega_2-\Omega}$ were also discarded because they lead to phase space displacement, which does not change entanglement properties. Moreover, they will typically average to zero, since they do not satisfy phase matching. The total Hamiltonian is given by the sum of the contributions for each positive frequency Ω, as $\hat{H}_\chi = \int_\epsilon^\infty \hat{H}_\chi(\Omega)d\Omega$. Therefore, the detailed treatment of the state of the sideband modes associated with a single analysis frequency Ω is decoupled from those of frequencies $\Omega' \neq \Omega$ [17].

If the evolution of the system could be described just by the unitary operations in Eq. (2) and the cavity dynamics without spurious losses, the resulting state would be pure, with entanglement for each one of the 31 possible bipartitions in the above-threshold operation. Nevertheless, Brillouin scattering of carrier photons by phonons of the crystal should be taken into account for intense intracavity fields [18]. From the optomechanical Hamiltonian [19], an extra contribution to the Hamiltonian of the form below can be derived

$$\hat{H}_g(\Omega) = \sum_{n=0}^{2}\sum_{j=1}^{3} -\hbar g_{nj}[\alpha_{\omega_n}(\hat{a}^{(n)\dagger}_{\omega_n-\Omega}\hat{d}^{(j)\dagger}_{\Omega} + \hat{a}^{(n)\dagger}_{\omega_n+\Omega}\hat{d}^{(j)}_{\Omega}) + \text{H.c.}], \tag{3}$$

with $\hat{d}^{(j)}_{\Omega_m}$ as the phonon annihilation operator on the mode of frequency Ω_m in longitudinal and transverse mechanical modes indicated by index j. It will couple the sideband modes to different thermal reservoirs of the crystal, thus degrading purity and entanglement even for perfect cavities. This phonon coupling appears to be intrinsic to the system, but it can, in principle, be mitigated by cooling down the crystal [8].

Therefore, the state of the sidebands depends on the mean fields and it can be directly related to the normalized pump power σ [20] for exact resonance, taking the oscillation threshold as $\sigma = 1$. Variation of this single parameter enables the exploration of this rich structure of nonclassical fields. Moreover, since only bilinear terms are involved, the resulting state is Gaussian, as experimentally observed in [21].

Entanglement is directly generated by the two-mode squeezing operator, associated with the creation and annihilation of photon pairs in different modes, presented in Eq. (2). This term is the only one remaining in subthreshold operation, leading to squeezed states or entanglement [4,6], coupling separate pairs of sidebands (Fig. 2). Above threshold, as the mean field of the down-converted modes grows with the increasing pump power, the coupling of the entangled modes to sidebands of the pump by the beam-splitter operators will transfer information to these modes and couple the formerly independent pair of entangled

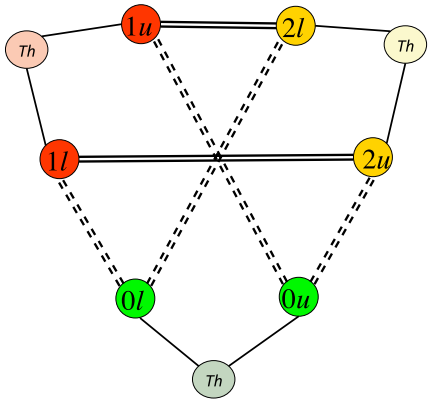

FIG. 2. Coupling of the six sideband modes of the field. Signal and idler sidebands are coupled by photon pair creation (and annihilation) operators (double lines). All the other modes are pairwise coupled by beam-splitter operations (double dashed lines). Each sideband pair is coupled to thermal reservoirs (Th) by phonon scattering (straight single lines). Notation: iu (il) stands for upper (lower) sideband modes at frequency $\omega_i + \Omega$ ($\omega_i - \Omega$).

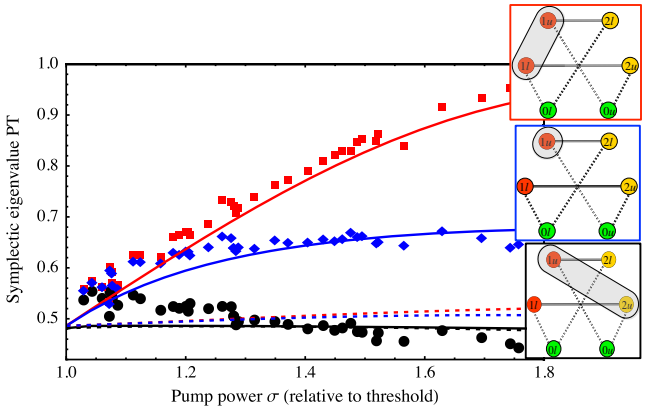

FIG. 3. Symplectic eigenvalues from the transpositions of different bipartitions. Experimental results are compared with the complete model (straight lines) and the model without phonons (dashed). (Inset) The modes selected for one partition are marked by the gray shadow.

states. The system would remain pure, but the coupling to the phonon modes, and the loss of information in their reservoirs, degrades information in the system as the power grows, as can be seen from Eq. (3).

In what follows, we study the OPO described in [17], using a potassium titanyl phosphate crystal inside a cavity with a free spectral range of 4.3(5) GHz and finesses of 15 for the pump mode and 125 for signal and idler modes. Transmittance of cavity mirrors is 30% for the pump and 4% for the infrared couplers. We performed a complete measurement of the covariance matrix of the Hermitian quadrature operators $(\hat{p}, \hat{q})$ of the field, associated with the annihilation operator $\hat{a} = \hat{p} + i\hat{q}$, for all the six modes involved, with overall quantum efficiencies of 65% for the pump and 87% for the infrared [22]. Entanglement in this system is observed by the analysis of the physicality of the smallest symplectic eigenvalue $\tilde{\nu}$ of the covariance matrix for a partially transposed density operator of the state [31]. Whenever $\tilde{\nu} < 1$, there is entanglement between the bipartitions [22]. Experimental results are presented in Figs. (3) and (4), confronted with the calculated values derived from our complete model of the OPO [17] (straight lines) and those without the phonon coupling (dashed lines). We have selected five representative cases from the complete set of results, which can be found in the Supplemental Material [22].

We begin the analysis by those bipartitions where the originally entangled modes lie in separate bipartitions, in Fig. 3. We can take both upper sidebands of signal and idler in one partition (black), both sidebands of the same field in one partition (red), or select a single sideband in one partition (blue). In all these situations, in the absence of phonons, the symplectic eigenvalue remains nearly unchanged for growing pump powers. A small change is observed in the second and third case as the power increases, indicating a transfer of information to the sidebands for the pump. Nevertheless, if we include those sidebands in the selected partition [22], deviations from this behavior are small.

The situation changes dramatically in the presence of phonons. The growing coupling of the entangled modes to thermal reservoirs degrades the entanglement for some bipartitions, eventually leading to separability [8]. It is interesting to notice that taking pairs of sidebands of different beams in the same partition provides a protected configuration (Fig. 3, black). This situation resembles the robustness of the twin beam squeezing [32], originated from the parity in the photon creation in the down-converted modes. On the other hand, if both sidebands from the same mode are taken in the same partition, phonon scattering leads to fast degradation of entanglement (Fig. 3, red). The difference between these cases can be understood from the fact that the coupling of each field to a thermal reservoir implies in correlated noise injected on the sidebands of that particular field, as a random phase modulation of the central carrier [18]. If we consider bipartition of the kind $1u2u \times 1l2l$, additional noise in mode $1u$ is correlated to the noise added in mode $1l$; therefore, information in both partitions remains correlated. The same applies to modes $2u$ and $2l$. On the other hand, for bipartitions of the kind $1l1u \times 2l2u$, fluctuations in mode 1 are not perfectly correlated to those of mode 2, and this additional noise degrades the overall correlation, leading to a reduction on the observed entanglement. It is curious to notice that, if we take just one of the modes in the partition (Fig. 3, blue), we have an intermediate situation, since we are comparing it to a set of modes where just one of them remains strongly correlated.

The role of the pump sidebands and their coupling to the entangled pairs remained almost unnoticed in the cases studied in Fig. 3. However, they have an important effect in

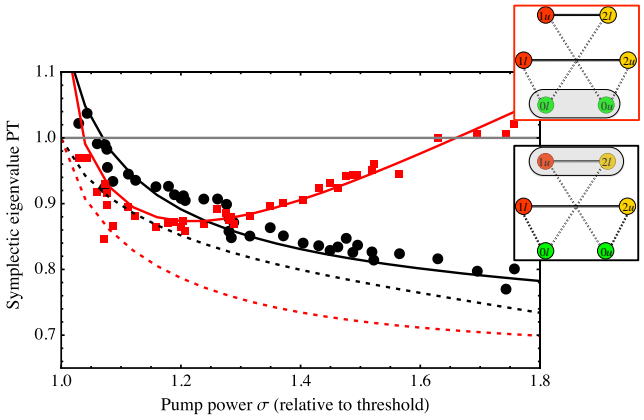

FIG. 4. Symplectic eigenvalues from the transpositions of different bipartitions. Experimental results are compared with the complete model (straight lines) and the model without phonons (dashed). (Inset) The modes selected for one partition are marked by the gray shadow.

other bipartitions for growing pump powers, as can be seen in Fig. 4. If we separate each pair of entangled modes in different partitions (Fig. 4, black), we have completely independent sets while operating below the threshold and therefore no entanglement between them. Above threshold, the signal and idler intensities are increased by growing pump power, and these pairs of modes are coupled to the pump sidebands [as can be seen in Eq. (2)], which intermediates the exchange of information between these two sets. The result is a growing entanglement between them that can be improved if the sidebands of the pump are evenly distributed between the bipartitions [22]. In the absence of phonon scattering, the result would be further improved, since the down-converted modes would be coupled to the same reservoir (the pump sidebands), whose evolution we can follow from the measurement of the pump.

The pump modes become necessarily entangled upon interaction with the signal and idler modes. In Fig. 4, the red curve shows the entanglement witness for the partition involving both pump sidebands. The observed entanglement is consistent with the one observed for an effective three-mode description of the OPO [8]. Once again, since the pump modes are coupled to the thermal reservoir of phonons, it suffers from the uncorrelated noise that is added to the sidebands and, as seen in the case of the single beam partition (Fig. 3, red), it is strongly affected in the case of intense intracavity fields, which grows with the pump power. The result is quite similar if we take only one of the sidebands in a 1×5 partition, as can be seen in the Supplemental Material [22].

The modes under study are selected by the choice of the demodulation frequency in the detection process. They are characterized by the analysis frequency, limited by the OPO cavity bandwidth (in the present case, in the range of 34 MHz), and the bandwidth of the detection or the measurement rate in the acquisition system (600 kHz). Different modes can be accessed just by changing the analysis frequency. All these independent hexapartite systems are simultaneously generated by a single monochromatic pump field. The present configuration of our system, detailed in the Supplemental Material [22], provides at least 20 sets of hexapartite entangled modes, each set independent from the other.

On the other hand, we can expect that, if multifrequency pump fields are used, with a frequency separation smaller than the cavity bandwidth, each intense pump mode can be treated classically by its mean value, and their fluctuations will now be coupled in the cavity in a situation similar to that shown in [11]. It opens the path to generate massive multipartite entanglement in this system from the multiple coupling of these hexapartite entangled states. Comparing to the other approaches [9,11,12], a similar large number of modes can be entangled. Here, we have the benefit of entangling sideband modes of carriers with very different wavelengths, enabling the distribution of quantum information over much broader, albeit discontinuous, bandwidths.

In conclusion, we have fully analyzed and characterized entanglement among six sideband modes in a triply resonant above-threshold OPO. The choice of the sidebands under study is done by the choice of the analysis frequency in the detected photocurrent. The rich structure of the entanglement generated can be easily controlled by means of the pump power, providing important flexibility for this platform. A controllable and scalable source of entangled states for quantum information tasks can thus be envisioned. The role of phonon scattering was also investigated, indicating that, by temperature control of the crystal, entanglement and purity of the system can be improved.

The authors acknowledge support from Grant No. 2010/08448-2, Fundação de Amparo à Pesquisa do Estado de São Paulo (FAPESP), Project No. 473847/2012-4 by the Conselho Nacional de Desenvolvimento Científico e Tecnológico, by the Instituto Nacional de Ciência e Tecnologia de Informação Quântica (INCT-IQ), and by Coordenação de Aperfeiçoamento de Pessoal de Nível Superior. M. Martinelli would like to thank Stephen P. Walborn for the discussions about the paper. The authors would like to thank the anonymous referees for fruitful suggestions that greatly contributed to a better presentation of the results.

*mmartine@if.usp.br

[1] M. A. Nielsen and I. L. Chuang, *Quantum Computation and Quantum Information* (Cambridge University Press, Cambridge, England, 2011).
[2] A. Einstein, B. Podolsky, and N. Rosen, Phys. Rev. **47**, 777 (1935).
[3] N. Bohr, Phys. Rev. **48**, 696 (1935).
[4] L. A. Wu, H. J. Kimble, J. L. Hall, and H. F. Wu, Phys. Rev. Lett. **57**, 2520 (1986).

[5] K. Kasai, G. Jiangrui, and C. Fabre, Europhys. Lett. **40**, 25 (1997); K. S. Zhang, T. Coudreau, M. Martinelli, A. Maître, and C. Fabre, Phys. Rev. A **64**, 033815 (2001).
[6] Z. Y. Ou, S. F. Pereira, H. J. Kimble, and K. C. Peng, Phys. Rev. Lett. **68**, 3663 (1992).
[7] A. S. Villar, L. S. Cruz, K. N. Cassemiro, M. Martinelli, and P. Nussenzveig, Phys. Rev. Lett. **95**, 243603 (2005).
[8] A. S. Coelho, F. A. S. Barbosa, K. N. Cassemiro, A. S. Villar, M. Martinelli, and P. Nussenzveig, Science **326**, 823 (2009).
[9] S. Yokoyama, R. Ukai, S. C. Armstrong, C. Sornphiphatphong, T. Kaji, S. Suzuki, J. Ichi Yoshikawa, H. Yonezawa, N. C. Menicucci, and A. Furusawa, Nat. Photonics **7**, 982 (2013).
[10] M. Pysher, Y. Miwa, R. Shahrokhshahi, R. Bloomer, and O. Pfister, Phys. Rev. Lett. **107**, 030505 (2011).
[11] M. Chen, N. C. Menicucci, and O. Pfister, Phys. Rev. Lett. **112**, 120505 (2014).
[12] J. Roslund, R. M. de Araújo, S. Jiang, C. Fabre, and N. Treps, Nat. Photonics **8**, 109 (2014).
[13] F. A. S. Barbosa, A. S. Coelho, K. N. Cassemiro, P. Nussenzveig, C. Fabre, A. S. Villar, and M. Martinelli, Phys. Rev. A **88**, 052113 (2013).
[14] A. Peres, Phys. Rev. Lett. **77**, 1413 (1996).
[15] M. D. Reid and P. D. Drummond, Phys. Rev. Lett. **60**, 2731 (1988); Phys. Rev. A **40**, 4493 (1989).
[16] F. A. S. Barbosa, A. S. Coelho, K. N. Cassemiro, P. Nussenzveig, C. Fabre, M. Martinelli, and A. S. Villar, Phys. Rev. Lett. **111**, 200402 (2013).
[17] L. F. Muñoz-Martínez, F. A. S. Barbosa, A. S. Coelho, L. Ortiz-Gutiérrez, M. Martinelli, P. Nussenzveig, and A. S. Villar, Phys. Rev. A **98**, 023823 (2018).
[18] J. E. S. César, A. S. Coelho, K. N. Cassemiro, A. S. Villar, M. Lassen, P. Nussenzveig, and M. Martinelli, Phys. Rev. A **79**, 063816 (2009).
[19] C. K. Law, Phys. Rev. A **51**, 2537 (1995).
[20] T. Debuisschert, A. Sizmann, E. Giacobino, and C. Fabre, J. Opt. Soc. Am. B **10**, 1668 (1993).
[21] A. S. Coelho, F. A. S. Barbosa, K. N. Cassemiro, M. Martinelli, A. S. Villar, and P. Nussenzveig, Phys. Rev. A **92**, 012110 (2015).
[22] See Supplemental Material at http://link.aps.org/supplemental/10.1103/PhysRevLett.121.073601 for a detailed description of the setup, and the evaluation of the entanglement witness for all the 31 possible bipartitions of the system, which includes Refs. [23–30].
[23] P. Galatola, L. Lugiato, M. Porreca, P. Tombesi, and G. Leuchs, Opt. Commun. **85**, 95 (1991).
[24] A. S. Villar, Am. J. Phys. **76**, 922 (2008).
[25] K. N. Cassemiro and A. S. Villar, Phys. Rev. A **77**, 022311 (2008).
[26] E. Schrödinger, Ber. Akad. Wiss. Berlin **24**, 296 (1930) [A. Angelow and M.-C. Batoni, Bulg. J. Phys. **26**, 193 (1999)].
[27] H. P. Robertson, Phys. Rev. **46**, 794 (1934).
[28] R. F. Werner and M. M. Wolf, Phys. Rev. Lett. **86**, 3658 (2001).
[29] G. Vidal and R. F. Werner, Phys. Rev. A **65**, 032314 (2002).
[30] G. Adesso, A. Serafini, and F. Illuminati, Phys. Rev. A **70**, 022318 (2004).
[31] R. Simon, Phys. Rev. Lett. **84**, 2726 (2000).
[32] A. Heidmann, R. J. Horowicz, S. Reynaud, E. Giacobino, C. Fabre, and G. Camy, Phys. Rev. Lett. **59**, 2555 (1987).